

PRELIMINARY CONCERNS ABOUT AGRONOMIC INTERPRETATION OF NDVI TIME SERIES FROM SENTINEL-2 DATA: PHENOLOGY AND THERMAL EFFICIENCY OF WINTER WHEAT IN PIEMONTE (NW ITALY)

Farbo A.^{a*}, Sarvia F.^a, De Petris S.^a, Borgogno-Mondino E.^a

^aDepartment of Agriculture, Forestry and Food Sciences, University of Torino, Grugliasco (TO), 10095, Italy

*Corresponding author: alessandro.farbo@unito.it

Commission III, WG III/10

KEY WORDS: TELECER Project, Winter Wheat, Crop Characterisation, NDVI Time Series, Crop Phenological Metrics, Growth Degree Day.

ABSTRACT:

TELECER project is supported through Rural Development Programme regional action of EU CAP and is aimed at providing Precision Agriculture–devoted services for cereals monitoring in the Piemonte Region (NW-Italy) context. In this work authors explored some general and preliminary issues mainly aimed at demonstrating and formalizing those evident relationships existing between NDVI image time series and the main ordinary agronomic parameters, with special focus on phenology and thermal efficiency of crops as related to Growing Degrees Day (GDD). Winter wheat was investigated and relationships calibrated at field level, making possible to spatially characterise environmental and management effects. Two different analysis were achieved: (i) one aimed at mapping crop phenological metrics, as derivable from NDVI S2 time series; (ii) one aimed at locally modelling relationship linking GDD and NDVI to somehow test the thermal efficiency of crops in the different parts of the study area. The first analysis showed that the end of season appears to be the most constant phenological metric in the study area possibly demonstrating a time concentration of harvest operations in the area. Differently, the peak of season and the start of season metrics showed to be largely varying in the study, thus suggesting to be stronger predictors: (i) of crop development; (ii) of the effects induced by local agronomical practices. Several base temperatures were used to compute correspondent GDD. These were tested against NDVI and modelled by a parabolic model at field level. Model coefficients distribution were analysed and mapped the correspondent agronomic interpretation suggested.

1. INTRODUCTION

1.1 Sentinel-2 Data in Agriculture

For the last years, Earth Observation (EO) data have been supporting many human activities including agriculture. In this context, the Sentinel-2 (S2) mission of the European Copernicus programme, providing high-resolution optical imagery for land monitoring purposes (Kuc and Chormański, 2019; Phiri et al., 2020), plays a key role. Starting from the S2 imagery several spectral vegetation index (VI) can be computed able to retrieve vegetation-related information at the proper spatial scale. The Normalized Difference Vegetation Index (NDVI), that combine RED (S2 - band 4) and NIR (S2 - band 8) bands, is widely used in agriculture (Huang et al., 2021). In particular, NDVI-based applications in agriculture include: crop phenology monitoring (Boori et al., 2019; Misra et al., 2020; Testa et al., 2018); crop yield estimation (Parida et al., 2021; Rahman and Robson, 2020; Zhao et al., 2020); crop nitrogen content estimation (Clevers and Gitelson, 2013; Sharifi, 2020); disaster events monitoring (Caballero et al., 2019; De Petris et al., 2021); risk management (Bacchini and Miguez, 2015); insurance activities for damage estimation (Sarvia et al., 2020; Shrestha et al., 2017); CAP controls in agriculture (Kanjir et al., 2018; Sarvia et al., 2021c). Additionally, S2 VIs have been applied in precision agriculture (PA) (Epinat et al., 2001; Ma et al., 2006; Sarvia et al., 2021b, p. 2). It is worth to remind that PA is a business management strategy that uses new technologies (sensors, processing software, machinery actuators) to support farmers decisions. In particular, PA adopts remotely-sensed data for many applications like pre-growth soil fertility and moisture

analyses, crop growth and yield forecasting (Sishodia et al., 2020). In this framework, S2 data well fit PA requirements due to its spectral (13 bands in the range 350-2500 nm), temporal (nominally 5 days) and geometric (10 m GSD, Ground Sampling Distance) resolutions (Segarra et al., 2020). Besides spectral approaches, several other methods can be used to retrieve vegetation-related information. Specifically, thermal data could be useful to explore physiological plant response. In fact, plants require a specific amount of heat to develop; consequently, one of the main driving phenological indicators can be found in the heat accumulated by vegetation during its growing season. The amount of heat energy that an organism accumulates can be expressed through the Growing Degree Day (GDD) (Durand et al., 1967). Thanks to the increasing adoption of meteorological sensors (temperature, rain, etc.), GDDs are currently and widely used in agrometeorological models to describe plant phenology (Ghamghami et al., 2019). Currently, several services and platforms have been developed by private companies combining S2 data with meteorological and ground data aiming at supporting the agricultural context. These platforms are expected to simplify and optimize farmers' work and to improve environmental and economic sustainability of their activities. Specifically, services concern: a) GIS-based field mapping, b) satellite-based crop monitoring, c) generation and delivery of crop disease prevention models, d) production and delivery of decision support systems; e) weather data analysis. The most of them are supplied by the Internet like OneSoil, Agrivi, FarmsLogs, Agrimap Crop Monitoring, Agriculus, Arvatec, FarmB.sat. Unfortunately, these services are not free of charge and the information they provide is uncertified. Moreover, they operate globally, with no neglecting

to adopt specifications related to local agronomic conditions and crop calendars. According to Aletdinova (Aletdinova and Lenski, 2021) main existing platforms releasing services, do not consider optimization models thus limiting farmers in obtaining possible solutions/suggestions based on real-time data. Moreover, these services suffer from two main limitations: (i) phenological metrics (PMs) are often neglected in data processing, when, differently, they can significantly improve data interpretation; in fact, PMs are able to summarize complex information about crop conditions, highlighting local anomalies that can be useful for crop management; (ii) data are processed through pre-trained models whose capability of generalization is hard to be demonstrated given the high variability of local conditions that can affect crop developments. These limitations raise some doubts about the general applicability of such services in heterogeneous agricultural contexts where spatial and temporal variability of meteorological, soil and agronomical conditions are significant. Consequently, they are difficult to be easily accepted by farmers. Given these premises, the TELECER (hereinafter called TELE) project titled “Productive and qualitative improvement of cereals cultivation within an advanced supply chain based on remote sensing” was launched in 2020 January. Within this project, Farmers’ Consortia (Piemonte Agricultural Consortium for Agri-Food and Cereals - CAPAC), Universities (Department of Agricultural, Forest and Food Sciences - DISAFA) and software companies were involved in developing and providing a shared, official and certified service for cereals (and maize) detection and monitoring. TELE is founded through the Regione Piemonte – PSR 2014-2020, 16.1.1 Action 2 (namely 2014IT06RDRP009: Italy - Rural Development Programme). TELE is in charge of developing a service combining satellite, meteorological and field data for crop monitoring (wheat, barley, corn and soybean) easy to be accessed by farmers. Information from the service is intended for addressing field agro-technical management practices like irrigation, fertilization and defence, with special focus on environmental conditions of the Piemonte region (NW Italy). Several local farmers were included in the project for a major sharing of problems, requirements and technical limitations that should guarantee a better compliance of the final service with robustness, reliability, effectiveness, simplicity and usability criteria.

1.2 Goals

This preliminary study is aimed at testing applicability of S2 time series for phenology and crop thermal efficiency description of winter-wheat (WW) in Piemonte region (NW-Italy) trying to figure out specific spatial patterns that could be related to environmental and management factors. In particular, starting from S2 and meteorological data, local models and phenological metrics were derived and calibrated for WW. Two different analyses were performed: (i) one aimed at mapping crop phenological metrics, as derivable from NDVI S2 time series; (ii) one aimed at locally modelling the well known relationship linking growing degree days (GDD) and NDVI (Borgogno-Mondino et al., 2020) somehow testing thermal efficiency of crops in the different parts of the study area.

2. MATERIALS AND METHODS

2.1 Study Area

Efficiency and robustness of crop monitoring by remote sensing strictly depends on the size of the observed field with respect to the image GSD (Meier et al., 2020; Vajsová et al., 2020). Consequently, only WW fields having a size > 0.1 ha (at least

10 S2 pixels @10 m GSD) were selected. A total of 47 WW fields were provided as a vector map by CAPAC local consortium (TELE partner) and used as ground reference data where crop and management type were known. Reference fields are located in the flat area of Piemonte, spreading across the entire region (Fig. 1). Piemonte is highly devoted to cereal production, producing about 11% of Italian wheat (Borri and Trione, 2020). Since Italy shows a high climatic variability depending on latitude, crop phenology management calendars change significantly region by region. For this reason, the Piemonte agronomic calendar was acquired (Sarvia et al., 2021c) showing that WW growing season starts in late October (sowing) and concludes on early July (harvesting) having its maximum phenological expression between April and May.

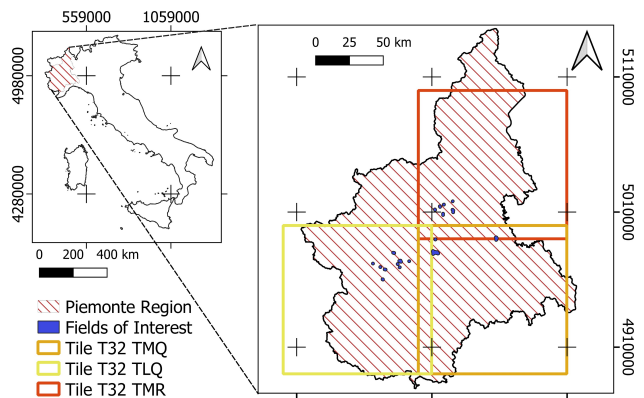


Figure 1. Piemonte Region (red lined) location in Italy.

Reference fields are represented by blue polygons. Orange/yellow/red squares border S2 tiles (Reference System: WGS84/UTM 32 N).

2.2 Sentinel-2 Data

In this work 22 S2 images were obtained ranging from 2nd November 2020 to 20th July 2021 (Figure 2). Images were obtained as Level 2A products (orthorectified and at-the-ground reflectance calibrated) from the Scientific Open Data Hub (<https://scihub.copernicus.eu/>). S2 data are provided as tiles of 100 x 100 km². According to WW spatial distribution, 3 tiles were needed, namely T32TMR, T32TMQ and T32TLQ (Fig 1) to cover the entire area. It is worth to remind that S2 Level 2A data are supplied together with a scene classification layer (SCL) alerting about cloudy, shadowy and fault pixels that is often used to detect and remove bad observations from the processed image time series. S2 technical features are reported in Table 1.

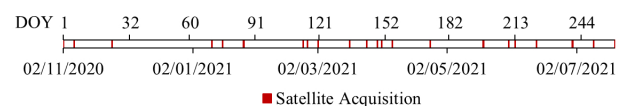


Figure 2. Acquisition date and DOY (day of the year) of the available S2 L2A images.

Spectral Band	Central Wavelength	Band Width	GSD
B1 (Aerosol)	443	20	60
B2 (Blue)	490	65	10
B3 (Green)	560	35	10
B4 (Red)	665	30	10
B5 (Red Edge 5)	705	15	20
B6 (Red Edge 6)	740	15	20
B7 (Red Edge 7)	783	20	20
B8 (Near Infrared)	842	115	10
B8A (Near Infrared Plateau)	885	20	20
B9 (Water Vapor)	945	20	60
B10 (Cirrus)	1380	30	60
B11 (Short Wave Infrared 1)	1610	90	20
B12 (Short Wave Infrared 2)	2190	180	20

Table 1. S2 MSI bands technical specifications: central wavelength, band width and ground sample distance (GSD).

2.3 Meteorological data

Since one of the goals of this work was to test and describe thermal efficiency of WW by relating GDD (eq. 3) with NDVI, the daily average air temperature was needed. Consequently, meteorological data were obtained from 11 meteorological stations (figure 3) belonging to the regional meteorological network (www.arpa.piemonte.it, last access 15th October 2021) located close to WW fields. Data were obtained for the period 2nd November 2020 - 30th June 2021 with daily frequency for a total of 280 temperature values.

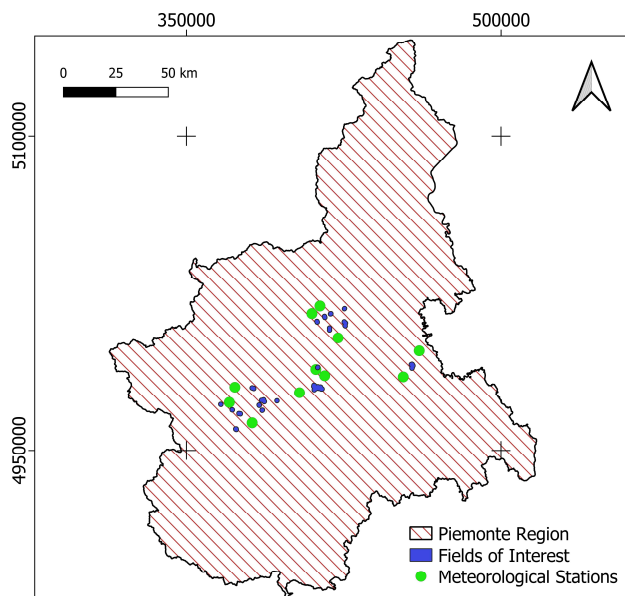


Figure 3. Meteorological Stations taken into account for the study. (Reference System: WGS84/UTM 32 N).

3. DATA PROCESSING

3.1 NDVI Time Series

According to its well-known capability of describing crop phenology and in order to guarantee the highest geometric resolution, in this work NDVI was considered. Consequently, starting from the native S2 tiles the correspondent image stacks of band 4 (red), band 8 (NIR) and SCL were generated. A self-developed routine was implemented in IDL v4.8 (Harris

Geospatial Solutions, Inc., Broomfield, CO, USA) (Chen et al., 2004) to generate NDVI times series for the reference period according to the following steps operating at pixel level: (i) bad observations were masked out according to SCL classification code; (ii) local NDVI temporal profile was interpolated by spline (tensor = 5) to obtain a regularized NDVI stack (5 day time resolution) made of 52 interpolated NDVI maps (for each processed tile). Finally, resulting NDVI stacks were mosaicked and the WW vector layer used to compute by zonal statistics the average NDVI temporal profile for WW fields.

3.2 Phenological Metrics Computation and Mapping

PM are useful to detect key moments along the growing season of vegetation (Misra et al., 2020) able to synthesize the entire cycle. For this work the following PM were computed at field level with reference to the local average NDVI temporal profile: start of season (SOS, as DOY = Day of the Year); NDVI peak value (NDVIM) and the correspondent date (POS, as DOY); end of season (EOS, as DOY), length of season (LOS, as DOY difference), growing rate (GR, as ratio) and senescence rate (SR, as ratio).

NDVIM corresponds to the maximum NDVI value reached by the crop during the considered period as derivable from the average and regularized NDVI temporal profile of the considered field; POS correspond to the DOY when NDVIM is reached; SOS and EOS were computed through a threshold-based approach looking for the DOY when the local NDVI value reaches 0.5 before and after the NDVI peak respectively (Misra et al., 2020); LOS was computed as the difference between EOS and SOS informing about the length of the phenological season. Concerning GR and SR, they were computed according to Eq. 1 and 2.

$$GR = \frac{NDVIM - NDVI_{SOS}}{POS - SOS} \quad (1)$$

$$SR = \frac{NDVI_{EOS} - NDVIM}{POS - EOS} \quad (2)$$

where $NDVIM$ is the maximum NDVI value along the growing season; $NDVI_{SOS}$ is the NDVI value at SOS; $NDVI_{EOS}$ is the NDVI value at EOS. Some statistics were finally computed to synthesize phenological behaviour of monitored fields.

3.3 Computing GDD

Plant growth is highly related to air temperature conditions. Growing Degree Days (GDD) is a metric that is known to describe biomass growth during the phenological season accounting for the temperature effects on crops, somehow related to its thermal efficiency.

In this work daily GDD was computed according to eq. 3 (Mcmaster, 1997). Daily temperature values were obtained from the meteorological station closest to the considered field and used to compute GDD.

$$GDD = \sum_{i=1}^n (T_{ave}^i - T_{BASE}) \begin{cases} \text{if } T_{ave}^i > T_{BASE} \rightarrow (T_{ave}^i - T_{BASE}) \\ \text{if } T_{ave}^i < T_{BASE} \rightarrow (0) \end{cases} \quad (3)$$

where T_{ave}^i is the daily average temperature for the i -th observation; T_{BASE} is the nominal base temperature (crop dependent) defining the minimum temperature value activating the phenological development of vegetation (Salazar-Gutierrez et al., 2013). T_{BASE} selection is a largely discussed topic in literature (Gill et al., 2014; Miller et al., 2001; Salazar-Gutierrez et al., 2013; Shaykewich, 1995). T_{BASE} is a very complex factor depending on both the plant species and the cultivar (Salazar-

Gutierrez et al., 2013). Moreover, while working with winter cereals T_{BASE} is known to vary along the phenological stages. For winter wheat T_{BASE} ranges from 0°C to 5°C (Boogar et al., 2013; Fraisse and Paula-Moraes, 2018; Salazar-Gutierrez et al., 2013; Shaykewich, 1995), making this choice not unique. Consequently, in order to assess the most suitable T_{BASE} for WW, three T_{BASE} were considered: (a) $T_{BASE} = 0$; (b) $T_{BASE} = 5$; (c) $T_{BASE} = 0$ before heading while $T_{BASE} = 5$ after heading until harvest. Thus, with reference to the available meteorological data, three different GDD profiles (namely GDD_0, GDD_5, GDD_05) were generated for each WW field corresponding to the three above mentioned T_{BASE} values. Depending on the different T_{BASE} , GDD profiles of crops show different growing rates. Specifically, lower T_{BASE} correspond to crops that grow along the winter season; higher T_{BASE} reflect a phenological stop in winter time and a slower overall growth.

3.4 NDVI vs GDD

Literature refers about a high correlation between GDD and NDVI (de Beurs and Henebry, 2004) being the former related to the cause and the latter to the effect of vegetation growing. In particular, a parabolic model demonstrated to well fit this relationship (eq. 4), assuming NDVI as predicted variable and the correspondent GDD as predictor one.

$$NDVIG = a \cdot GDDC^2 + b \cdot GDDC + c \quad (4)$$

where a , b and c are the model coefficients estimated by ordinary least squares.

Consequently, the parabolic model of eq. 4 was calibrated separately for each of the available WW fields. Model calibration was obtained including only those observations showing, contemporarily, an NDVI value > 0.3 (i.e. active vegetation) and a $T_{ave}^i > T_{BASE}$. The calibrated local model was used to obtain the expected NDVI value ($NDVIG$) related to thermal effects. Was then calculated as reported in Equation (4) (Borgogno-Mondino et al., 2020; de Beurs and Henebry, 2004; Walker et al., 2015) for each WW and considering the 3 different T_{BASE} . Models related to the different T_{BASE} were compared and their performance evaluated by the standard error of estimates (SEE, (Gonçalves and White, 2005)) and the mean absolute errors (MAE, (Willmott and Matsuura, 2005)).

Subsequently, a new index called $NDVIG_{MAX}$ was computed (eq.5) in order to better describe the phenological peak as predicted by temperature data.

$$NDVIG_{MAX} = c - \frac{b^2}{4a} \quad (5)$$

where $NDVIG_{MAX}$ is the maximum $NDVIG$ as predicted by the quadratic model.

Finally, the differences between $NDVIG_{MAX}$ and $NDVIM$ were calculated at field level.

4. RESULTS

4.1 Phenological Metrics

Once PM were computed at field level, statistical distribution (Fig. 4) of SOS, EOS, POS, LOS and $NDVIM$ from WW fields were analysed in order to qualify and characterize fields within AOI. Based on boxplots following considerations can be carried out: (a) average WW SOS is placed at 6th observation with a fairly high variability, which means that SOS starts around at 27th November fitting expected local agronomical calendar

(Sarvia et al., 2021b); (b) average WW EOS is placed at 46th observation with a low variability, which means that EOS ends at 15th June in almost all cases; (c) average WW LOS is equal to 39 observations with a fairly high variability, which means that LOS persist around 195 days. (d) average WW POS is placed at 35th observation with a fairly high variability, which means that POS occurs around 21st April. (e) average WW $NDVIM$ is equal to 0.83 with a fairly high variability.

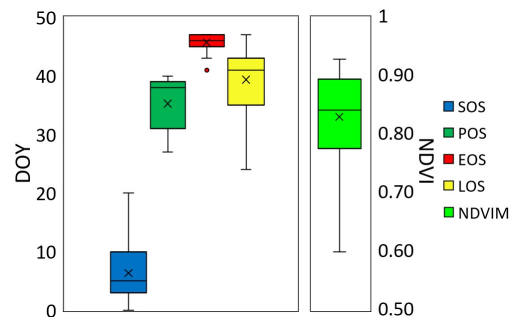


Figure 4. Boxplots of PMs. Bottom-up: 5th, 25th, 50th, 75th and 95th percentiles. Cross is the PM mean value. Dots are outliers.

These results appear to be consistent and supported by the local climatic, environmental and agricultural conditions. SOS high variability can be interpreted as related to farmers' technical choices and, in particular, with the sowing date of each field. Conversely, EOS low variability can be associated to the ripening and maturity stages that usually occur at similar dates (June) in AOI. Consequently, LOS high variability can be associated mostly to the one that SOS suffers from. The high variability of $NDVIM$ and POS are probably due to WW different agricultural, meteorological and environmental local conditions that can positively, or negatively, affect crop development. It is worth to remind that the most relevant drivers that could influence NDVI (and therefore crop development) are: soil type, nutrients, pathologies, water availability and terrain aspect (Neenu et al., 2013). As far as GR and SR are concerned, the correspondent statistical distributions were computed and summarized in the boxplots of figure 5. Averagely, GR was found to be 0.12 with very low variability; this means that WW growth tends to be quite similar in the monitored fields. This result is consistent with winter crop phenological development which is characterized by slower growth (GR), probably due to winter low temperatures within AOI. Conversely, the average SR value was found to be -0.04 with fairly high variability. This result can still be related to crop reaction to environmental conditions, leading to significant variations within crop development and maturity.

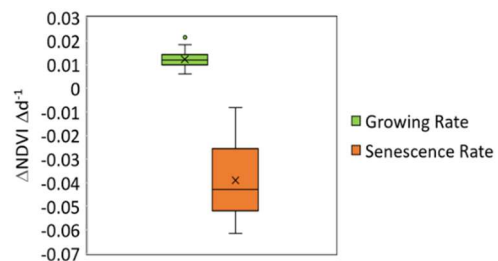


Figure 5. GR and SR metrics for WW fields. Bottom-up: 5th, 25th, 50th, 75th and 95th percentiles. Cross is the PM mean value. Dots are outliers.

4.2 GDD Computation

As previously stated, GDD profiles strongly depend from T_{BASE} . Figure 6 shows the average GDD profiles corresponding to the three considered T_{BASE} values, as computed with reference to the whole WW dataset.

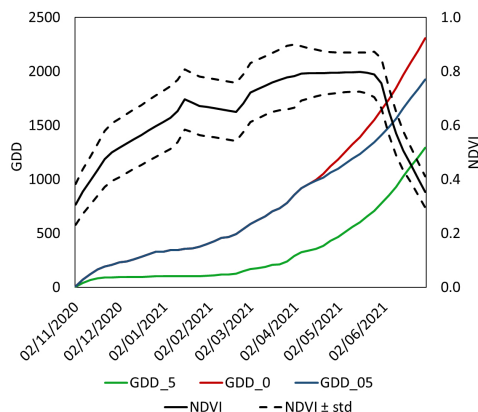


Figure 6. GDD profiles (GDD_5, GDD_0, GDD_05) as computed with reference to the three considered T_{BASE} values. NDVI and GDD profiles are the average ones from the whole WW dataset.

Looking at figure 6 it can be noted that GDD_0 profile continues its growing even in winter time without long pause periods. Conversely, GDD_5 profile appears to stop its growing from December to early March. As far as GDD_05 profile is concerned it looks similar to the GDD_0 one in its early phase (until April); after, it slows down assuming a slope similar to the GDD_5 one. These differences highlight that a high degree of uncertainty is present depending on the selected model. A more objective way for selecting the proper model is therefore mandatory. The possibility of testing NDVI vs GDD correlations is certainly one of the possible tool for obtaining the answer to this question (see next section).

Further looking at figure 6, on 30th June (last observation) the following thermal sums can be found: 1294, 2309 and 1926 for GDD_5, GDD_0 and GDD_05, respectively. These values appear to be consistent with the ones from literature. Both GDD_0 and GDD_5 show final values similar to those reported in (Salazar-Gutierrez et al., 2013) for Georgia, USA and in (Gill et al., 2014) for the Punjab region, India. Concerning GDD_05, no study was found in literature to support or contradict our results.

4.3 NDVI as a function of GDDC

To find which T_{BASE} was more suitable for the AOI fields, the three GDD profiles were tested against NDVI. According to eq. 4, a parabolic model was calibrated for each WW field (47) and for all the three considered GDD profiles. A total of $47 \times 3 = 141$ models were calibrated. Correspondent SEE were computed and separately analysed for the three GDD profiles (Fig 7).

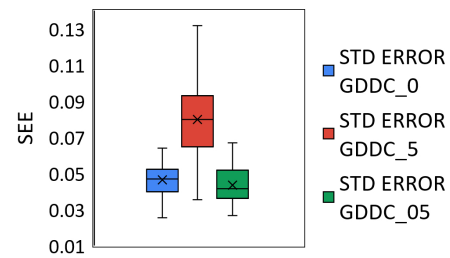


Figure 7. SEE statistics as computed from the calibrated parabolic models relating local NDVI and GDD. They refer to the GDD_5, GDD_0 and GDD_05 profiles. Bottom-up: 5th, 25th, 50th, 75th and 95th percentiles. Cross corresponds to the mean value.

Figure 7 shows that the lowest SEE mean value (0.043) corresponds to the model that uses the GDD_05 profile as NDVI predictor. A similar performance in terms of SEE mean value was achieved with reference to the GDD_0 profile (0.047). Differently, GDD_5 proved to be a worse predictor determining a SEE mean value of 0.079.

As far as representativeness of SEE mean value is concerned, it was possible to note that the one associated to GDD_0 was the higher one (lower standard deviation = 0.009855) even if weakly better of the one from GDD_05 (standard deviation = 0.010056); additionally, GDD_0 SEE distribution appeared to be less skewed (skewness = -0.148) than the one from GDD_05 (Skewness = 0.309), having a favourable skewness compacting higher SEE values against its mean value. On the other side, unreliability of NDVI prediction by GDD_5 is confirmed by the correspondent highest standard deviation (0.023). Taking care of these evidences, it can be stated that, in AOI, a T_{BASE} of 5 °C has to be absolutely, avoided. Some doubts persist about the performances given by GDD_0 and GDD_05 profiles, that globally appear to be very similar. Nevertheless, a preliminary evaluation based on the above mentioned criteria, addressed us to consider GDD_0 as the best choice, in spite of the slightly higher SEE mean value. A final and decisive selection could however come by comparing the performance (Mean Absolute Error – MAE, figure 8) of the GDD_05 and GDD_0 in the last part of the growing season where the two profiles diverge (16th April - 30th June).

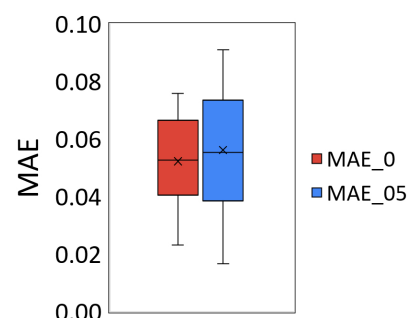


Figure 8. MAE of the GDD_0 and GDD_05 models (MAE_0 and MAE_05 respectively) in the period 6th April - 30th June.

Figure 8 showed that GDD_0 model leads to lower mean and standard deviation MAE values (0.052 and 0.015 respectively) than GDD_05 (0.056 and 0.021 respectively), denoting a slight difference between the two models; consequently, $T_{BASE}=0$ was chosen as the reference one for this work.

Once the optimal T_{BASE} was defined, GDD_0-based model coefficients distributions (a , b and c) were analysed (Fig. 9). It is worth to remind that: c coefficient defines the model offset; b is mainly related to function maximum/minimum and slope in the variable space; a majorly conditions both slope and

concavity (higher absolute values correspond to a narrower concavity). As previously reported in Eq. (5), a and b concur in determining the model maximum/minimum.

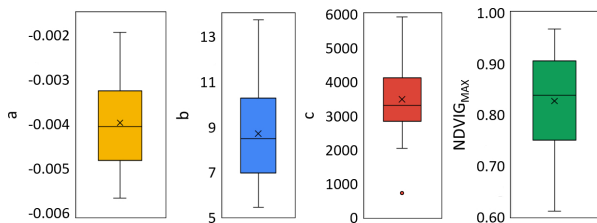


Figure 9. Boxplots representing the statistical distribution of the three GDD₀-based model coefficients (a , b , c) and the NDVIG_{MAX} predicted by the model. From bottom-up: 5th, 25th, 50th, 75th and 95th percentiles. Cross is the mean value. Dots are outliers. All coefficients are multiplied by 10000.

Figure 9 shows that mean values were 3500, 8.7 and -0.004 for c , b and a respectively; it is worth to remind that all coefficients are multiplied by 10000.

In particular, c value is consistent with the NDVI value corresponding to the begin of WW development (0.3); b values result to be quite low due to long growth period and low winter temperatures; a values result to be always negative confirming that NDVI decreases after reaching its peak (Sarvia et al., 2021a).

Concerning the possible agronomic meaning of model coefficients, the following interpretation can be given: (i) c , being related to the initial NDVI values could depend on several agronomical drivers like crop seeding and emergence time, local pedological features and genetic differences of cultivars; (ii) a and b , defining the increase of NDVI as a function of GDD, could be used to summarize the strength of WW development and, consequently, its thermal efficiency. Additionally, a refers about length of vegetation activity before harvesting. Summarizing, it can be stated that the c coefficient is completely related to the early stages of development and in particular, mainly influenced by the sowing period. Conversely, a and b seem to be related to the growing season and in particular to the growing rate. To give an operational demonstration of the generated information a small focus area (FA) was chosen and mapped. In particular the spatial variability of coefficients (Figure 10), NDVIG_{MAX}, NDVIM and their difference (Figure 11) were mapped. Distribution of coefficients showed a great variability within FA, suggesting that they can be adopted for WW characterization according to the previously provided interpretation keys. For example, concerning the c coefficient of figure 10a, it can be noted that some fields showed values lower than 1000 suggesting that in November no vegetative activity was on and, therefore, that WW was not still in its emergence phase. Conversely, other fields showed values greater than 5000, proving that a weak vegetative activity was on and, therefore, that WW had already started its emergence phase. Concerning other coefficients, in FA high b and a absolute values were located where WW showed low c values. This suggest that a rapid growth rate occurred in these fields trying to compensate emergence delays. Additionally, some fields showed intermediate values of b and a suggesting that crop development was more constant.

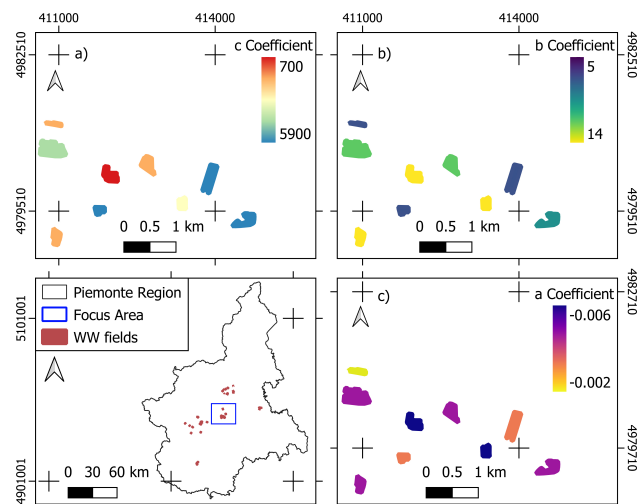


Figure 10. a , b and c coefficients' spatial variability within a focus area in Piemonte Region. (Reference System: WGS84/UTM 32 N).

As far as the relationship between PM and GDD-related estimates is concerned, NDVI peak is known to be a good predictor of crop yield (Sultana et al., 2014). Therefore, interesting outcomes can come by comparing NDVIG_{MAX} and NDVIM. Surprisingly, the two peaks showed different values and a different pattern in FA (Fig. 10). It is worth to remind that NDVIG_{MAX} is estimated through the GDD-based model, and it somehow refers about WW expected thermal efficiency. Differently, NDVIM is the NDVI maximum as seen by satellite and therefore it absorbs all environmental and agronomic factors affecting crop growth (soil, cultivar, water availability, agronomic management). Since differences between NDVIG_{MAX} and NDVIM ranged between 0.04 and 0.09 NDVI points (Fig. 11c), they can be retained significant (Borgogno-Mondino et al., 2016)). Consequently, they can be used to somehow recognize anomalies in thermal efficiency of WW that can be related to possible differences in yield.

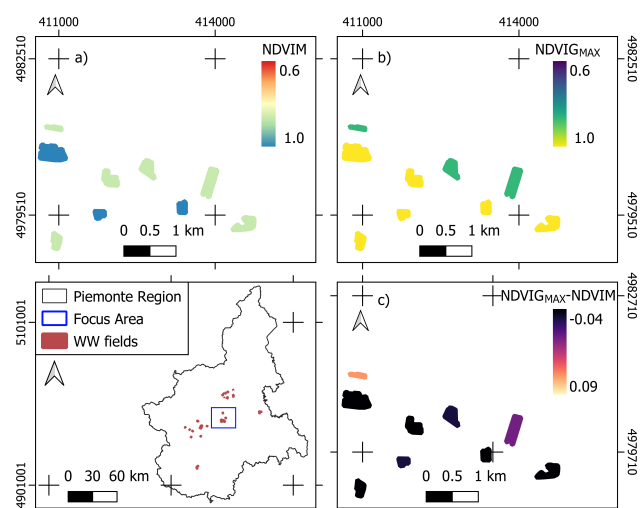


Figure 11. NDVIG_{MAX}, NDVIM and NDVIG_{MAX} – NDVIM spatial variability within a focus area in Piemonte Region. (Reference System: WGS84/UTM 32 N).

Due to the preliminary nature of this work, future developments will be conducted in order to relate these deductions to the yields and over other crops pertaining TELE (corn, barley, soybean, etc). The possibility of locally map this values, could

drive to interesting information useful for a proper and more sustainable management of crops in the area.

5. CONCLUSIONS

This work was developed within the TELECER project that is aimed at improving and supporting the cereal sector within the Piemonte region (NW Italy), through the adoption of Copernicus Sentinel-2 data. Presented results are preliminary and concern the characterization of winter wheat fields in the area managed by the CAPAC. To characterize winter wheat development, two different procedures were proposed: a) one based on phenological metrics derived by NDVI time series; in particular SOS, EOS, LOS, POS, NDVIM, GR and SR were computed at field level for winter wheat; b) one based on modelling of local relationships between growing degree days and NDVI to investigate local thermal efficiency of WW. The first analysis proved that EOS is the less variable phenological metric in AOI, suggesting a common WW behaviour during its maturity/harvesting. Differently, POS and SOS appeared to be the most variable phenological metrics in AOI, able to characterize WW development and agronomical practices (sowing) respectively. According to the second analysis, several T_{BASE} values were tested demonstrating that a T_{BASE} of 0°C is the most proper in AOI and that a parabolic model well fits the relationship between GDD and NDVI. It was also proved that model coefficients can be used to summarize local thermal efficiency of WW. Some agronomic interpretations were proposed about model coefficients; moreover, since they can be locally computed at field level, they can also be mapped giving new spatial information for a more proper sustainable management of WW in the area. This is a remarkable consideration especially when WW fields are managed/monitored unitarily through agronomic strategies based on Consortia, like CAPAC.

REFERENCES

- Aletdinova, A.A., Lenski, A.V., 2021. Information support for crop production automation in Russia and Belarus. *IOP Conference Series: Earth and Environmental Science*. IOP Publishing, p. 012058.
- Bacchini, R.D., Miguez, D.F., 2015. Agricultural risk management using NDVI pasture index-based insurance for livestock producers in south west Buenos Aires province. *Agricultural Finance Review*.
- Boogar, A.A.M., Nasiri, B., Pour, R.H., Zare, S., Alam, J.N., 2013. Determination of suitable date for wheat culture by data of climate: Case study Eghlid region. *Applied Botany* 62, 17434-17439.
- Boori, M.S., Choudhary, K., Paringer, R., Sharma, A.K., Kupriyanov, A., Corgne, S., 2019. Monitoring crop phenology using NDVI time series from sentinel 2 satellite data. *2019 5th International Conference on Frontiers of Signal Processing (ICFSP), IEEE*, 62–66.
- Borgogno-Mondino, E., de Palma, L., Novello, V., 2020. Investigating Sentinel 2 Multispectral Imagery Efficiency in Describing Spectral Response of Vineyards Covered with Plastic Sheets. *Agronomy* 10, 1909.
- Borgogno-Mondino, E., Lessio, A., Gomasasca, M.A., 2016. A fast operative method for NDVI uncertainty estimation and its role in vegetation analysis. *European Journal of Remote Sensing* 49, 137–156.
- Borri, I., Trione, S., 2020. L'AGRICOLTURA NEL PIEMONTE IN CIFRE 2020.
- Caballero, I., Ruiz, J., Navarro, G., 2019. Sentinel-2 satellites provide near-real time evaluation of catastrophic floods in the west mediterranean. *Water* 11, 2499.
- Chen, J., Jönsson, Per., Tamura, M., Gu, Z., Matsushita, B., Eklundh, L., 2004. A simple method for reconstructing a high-quality NDVI time-series data set based on the Savitzky–Golay filter. *Remote Sensing of Environment* 91, 332–344.
- Clevers, J.G., Gitelson, A.A., 2013. Remote estimation of crop and grass chlorophyll and nitrogen content using red-edge bands on Sentinel-2 and-3. *International Journal of Applied Earth Observation and Geoinformation* 23, 344–351.
- de Beurs, K.M., Henebry, G.M., 2004. Land surface phenology, climatic variation, and institutional change: Analyzing agricultural land cover change in Kazakhstan. *Remote Sensing of Environment* 89, 497–509.
- De Petris, S., Sarvia, F., Borgogno Mondino, E., 2021. Multi-temporal mapping of flood damage to crops using sentinel-1 imagery: a case study of the Sesia River (October 2020). *Remote Sensing Letters* 12, 459–469.
- Durand, R., De Parcevaux, S., Roche, P., 1967. Action de la température sur la croissance et le développement du lin. *Annales de Physiologie Végétale*, 87–105.
- Epinat, V., Stein, A., de Jong, S.M., Bouma, J., 2001. A wavelet characterization of high-resolution NDVI patterns for precision agriculture. *International Journal of Applied Earth Observation and Geoinformation* 3, 121–132.
- Fraisse, C.W., Paula-Moraes, S.V., 2018. Degree-days: growing, heating, and cooling. *EDIS*.
- Ghamghami, M., Ghahreman, N., Irannejad, P., Ghorbani, K., 2019. Comparison of data mining and GDD-based models in discrimination of maize phenology. *International Journal of Plant Production* 13, 11–22.
- Gill, K., Babuta, R., Kaur, N., SANDHU, S., 2014. Thermal requirement of wheat crop in different agroclimatic regions of Punjab under climate change scenarios. *Mausam* 65, 417–424.
- Gonçalves, S., White, H., 2005. Bootstrap Standard Error Estimates for Linear Regression. *Journal of the American Statistical Association* 100, 970–979.
- Huang, S., Tang, L., Hupy, J.P., Wang, Y., Shao, G., 2021. A commentary review on the use of normalized difference vegetation index (NDVI) in the era of popular remote sensing. *Journal of Forestry Research* 32, 1–6.
- Kanjir, U., \DJurić, N., Veljanovski, T., 2018. Sentinel-2 based temporal detection of agricultural land use anomalies in support of common agricultural policy monitoring. *ISPRS International Journal of Geo-Information* 7, 405.
- Kuc, G., Chormański, J., 2019. SENTINEL-2 IMAGERY FOR MAPPING AND MONITORING IMPERVIOUSNESS IN

- URBAN AREAS. *Int. Arch. Photogramm. Remote Sens. Spatial Inf. Sci.* XLII-1/W2, 43–47.
- Ma, Q., Chen, Q., Shang, Q., Zhang, C., 2006. The Data Acquisition for Precision Agriculture Based on Remote Sensing, in: 2006 IEEE International Symposium on Geoscience and Remote Sensing. *2006 IEEE International Symposium on Geoscience and Remote Sensing*, 888–891.
- McMaster, G., 1997. Growing degree-days: one equation, two interpretations. *Agricultural and Forest Meteorology* 87, 291–300.
- Meier, J., Mauser, W., Hank, T., Bach, H., 2020. Assessments on the impact of high-resolution-sensor pixel sizes for common agricultural policy and smart farming services in European regions. *Computers and Electronics in Agriculture* 169, 105205.
- Miller, P., Lanier, W., Brandt, S., 2001. Using growing degree days to predict plant stages. *Ag/Extension Communications Coordinator, Communications Services, Montana State University-Bozeman, Bozeman, MO* 59717, 994–2721.
- Misra, G., Cawkwell, F., Wingler, A., 2020. Status of phenological research using Sentinel-2 data: A review. *Remote Sensing* 12, 2760.
- Neenu, S., Biswas, A.K., Rao, A.S., 2013. Impact of climatic factors on crop production-a review. *Agricultural Reviews* 34, 97–106.
- Parida, B.R., Kumar, A., Ranjan, A.K., 2021. Crop Types Discrimination and Yield Prediction Using Sentinel-2 Data and AquaCrop Model in Hazaribagh District, Jharkhand. *KN-Journal of Cartography and Geographic Information*, 1–13.
- Phiri, D., Simwanda, M., Salekin, S., Nyirenda, V.R., Murayama, Y., Ranagalage, M., 2020. Sentinel-2 Data for Land Cover/Use Mapping: A Review. *Remote Sensing* 12, 2291.
- Rahman, M.M., Robson, A., 2020. Integrating Landsat-8 and Sentinel-2 Time Series Data for Yield Prediction of Sugarcane Crops at the Block Level. *Remote Sensing* 12, 1313.
- Salazar-Gutierrez, M.R., Johnson, J., Chaves-Cordoba, B., Hoogenboom, G., 2013. Relationship of base temperature to development of winter wheat. *International Journal of Plant Production* 7.
- Sarvia, F., De Petris, S., Borgogno-Mondino, E., 2021a. Exploring Climate Change Effects on Vegetation Phenology by MOD13Q1 Data: The Piemonte Region Case Study in the Period 2001–2019. *Agronomy* 11, 555.
- Sarvia, F., De Petris, S., Borgogno-Mondino, E.C., 2020. Multi-scale remote sensing to support insurance policies in agriculture: from mid-term to instantaneous deductions. *GIScience & Remote Sensing* 57, 770–784.
- Sarvia, F., Petris, S.D., Orusa, T., Borgogno-Mondino, E., 2021b. MAIA S2 Versus Sentinel 2: Spectral Issues and Their Effects in the Precision Farming Context. *International Conference on Computational Science and Its Applications. Springer*, 63–77.
- Sarvia, F., Xausa, E., De Petris, S., Cantamessa, G., Borgogno-Mondino, E., 2021c. A Possible Role of Copernicus Sentinel-2 Data to Support Common Agricultural Policy Controls in Agriculture. *Agronomy* 11, 110.
- Segarra, J., Buchailot, M.L., Araus, J.L., Kefauver, S.C., 2020. Remote sensing for precision agriculture: Sentinel-2 improved features and applications. *Agronomy* 10, 641.
- Sharifi, A., 2020. Using sentinel-2 data to predict nitrogen uptake in maize crop. *IEEE Journal of Selected Topics in Applied Earth Observations and Remote Sensing* 13, 2656–2662.
- Shaykewich, C.F., 1995. An appraisal of cereal crop phenology modelling. *Can. J. Plant Sci.* 75, 329–341.
- Shrestha, R., Di, L., Yu, E.G., Kang, L., Shao, Y., Bai, Y., 2017. Regression model to estimate flood impact on corn yield using MODIS NDVI and USDA cropland data layer. *Journal of Integrative Agriculture* 16, 398–407.
- Sishodia, R.P., Ray, R.L., Singh, S.K., 2020. Applications of remote sensing in precision agriculture: A review. *Remote Sensing* 12, 3136.
- Sultana, S.R., Ali, A., Ahmad, A., Mubeen, M., Zia-Ul-Haq, M., Ahmad, S., Ercisli, S., Jaafar, H.Z.E., 2014. Normalized Difference Vegetation Index as a Tool for Wheat Yield Estimation: A Case Study from Faisalabad, Pakistan. *The Scientific World Journal*.
- Testa, S., Soudani, K., Boschetti, L., Mondino, E.B., 2018. MODIS-derived EVI, NDVI and WDRVI time series to estimate phenological metrics in French deciduous forests. *International journal of applied earth observation and geoinformation* 64, 132–144.
- Vajsová, B., Fasbender, D., Wirnhardt, C., Lemajic, S., Devos, W., 2020. Assessing Spatial Limits of Sentinel-2 Data on Arable Crops in the Context of Checks by Monitoring. *Remote Sensing* 12, 2195.
- Walker, J.J., de Beurs, K.M., Henebry, G.M., 2015. Land surface phenology along urban to rural gradients in the U.S. Great Plains. *Remote Sensing of Environment* 165, 42–52.
- Willmott, C.J., Matsuura, K., 2005. Advantages of the mean absolute error (MAE) over the root mean square error (RMSE) in assessing average model performance. *Climate Research* 30, 79–82.
- Zhao, Y., Potgieter, A.B., Zhang, M., Wu, B., Hammer, G.L., 2020. Predicting wheat yield at the field scale by combining high-resolution Sentinel-2 satellite imagery and crop modelling. *Remote Sensing* 12, 1024.